



THE UNIVERSITY *of* EDINBURGH

Edinburgh Research Explorer

Erosion-deposition patterns and depo-center movements in branching channels at the near-estuary reach of the Yangtze River

Citation for published version:

Zhu, B, Deng, J, Tang, J, Yu, W, Borthwick, AGL, Chai, Y, Sun, Z & Li, Y 2020, 'Erosion-deposition patterns and depo-center movements in branching channels at the near-estuary reach of the Yangtze River', *Frontiers of Earth Science*, vol. 14. <https://doi.org/10.1007/s11707-019-0808-2>

Digital Object Identifier (DOI):

[10.1007/s11707-019-0808-2](https://doi.org/10.1007/s11707-019-0808-2)

Link:

[Link to publication record in Edinburgh Research Explorer](#)

Document Version:

Peer reviewed version

Published In:

Frontiers of Earth Science

General rights

Copyright for the publications made accessible via the Edinburgh Research Explorer is retained by the author(s) and / or other copyright owners and it is a condition of accessing these publications that users recognise and abide by the legal requirements associated with these rights.

Take down policy

The University of Edinburgh has made every reasonable effort to ensure that Edinburgh Research Explorer content complies with UK legislation. If you believe that the public display of this file breaches copyright please contact openaccess@ed.ac.uk providing details, and we will remove access to the work immediately and investigate your claim.



**Erosion-deposition patterns and depo-center movements in
branching channels at the near-estuary reach of the Yangtze
River**

**Boyuan ZHU (✉)¹, Jinyun DENG², Jinwu TANG³, Wenjun YU⁴,
Alistair G.L. BORTHWICK⁵, Yuanfang CHAI⁶, Zhaohua SUN²,
Yitian LI²**

¹ School of Hydraulic Engineering, Key Laboratory of Water-Sediment Sciences and Water
Disaster Prevention of Hunan Province, Changsha University of Science & Technology, Changsha
410114, China

² State Key Laboratory of Water Resources and Hydropower Engineering Science, Wuhan
University, Wuhan 430072, China

³ Changjiang Institute of Survey, Planning, Design and Research, Wuhan 430010, China

⁴ Changjiang Waterway Institute of Planning, Design & Research, Wuhan 430040, China

⁵ School of Engineering, The University of Edinburgh, The King's Buildings, Edinburgh EH9
3JL, UK

⁶ Department of Earth Sciences, Vrije Universiteit Amsterdam, Boelelaan 1085, 1081 HV
Amsterdam, The Netherlands

E-mail: boyuan@csust.edu.cn

Abstract

Channel evolution and depo-center migrations in braided reaches are significantly influenced by variations in runoff. This study examines the effect of runoff variations on the erosion-deposition patterns and depo-center movements within branching channels of the near-estuary reach of the Yangtze River. We assume that variations in annual mean duration days of runoff discharges, ebb partition ratios in branching channels, and the erosional/depositional rates of entire channels and sub-reaches are representative of variations in runoff intensity, flow dynamics in branching channels, and morphological features in the channels. Our results show that the north region of Fujiangsha Waterway, the Liuhaisha branch of Rugaoshan Waterway, the west branch of Tongzhousha Waterway, and the west branch of Langshansha Waterway experience deposition or reduced erosion under low runoff intensity, and erosion or reduced deposition under high runoff intensity, with the depo-centers moving upstream and downstream, respectively. Other waterway branches undergo opposite trends in erosion-deposition patterns and depo-center movements as the runoff changes. These morphological changes may be associated with trends in ebb partition ratio as the runoff discharge rises and falls. By flattening the intra-annual distribution of runoff discharge, dam construction in the Yangtze Basin has altered the ebb partition ratios in waterway branches, affecting their erosion-deposition patterns and depo-center movements. Present trends are likely to continue into the future as a succession of large cascade dams is under construction along the upper Yangtze.

Keywords near-estuary reach, Yangtze River, runoff discharge, ebb partition ratio,

erosion-deposition pattern, depo-center movement

1 Introduction

Morphological evolution of river systems is important to river management and regulation, and has become a growing issue over the past decades (Li et al., 2014; Zhu et al., 2017; Schletterer et al., 2019). Braided reaches are commonplace in rivers, with alternate development and shrinkage occurring between the main stem and secondary branches; such reaches often extend from the head source to the estuary (Jain and Sinha, 2004; Latrubesse, 2008; Jansen and Nanson, 2010; Chen et al., 2016; Li et al., 2016; Han et al., 2018; Zhu et al., 2017, 2019). It has been established that differences in evolutionary processes between bifurcated branches are primarily caused by changes in lateral flow dynamics, driven by variations in flow discharge (i.e. upstream runoff discharge or downstream tidal discharge) (Chen et al., 2016; Han et al., 2018; Zhu et al., 2017, 2019), local human activities (e.g. channel improvement works, and sand excavation) (Kuang et al., 2014; Zheng et al., 2018; Dai and Ding, 2019), and Coriolis-induced circulation in estuarine areas (Wang et al., 2013; Li et al., 2011, 2014). Dams modulate runoff discharge in rivers worldwide and can drive the morphological evolution of braided reaches, as demonstrated by many inland rivers (Petts and Gurnell, 2005; Graf, 2006; Han et al., 2018; Alcayaga et al., 2019; Mendoza et al., 2019; Zhu et al., 2019) and estuarine areas (Warne et al., 2002; Sloff et al., 2013; Zhu et al., 2017; Liu et al., 2018; Zhou et al., 2018), noting that tidal discharges are relatively stable at the yearly time scale (Horrevoets et al., 2004; Jiang et al., 2012a; Zhu et al., 2017). For fluvial braided reaches, shrinking or developing trends of branching channels are often

aggravated or interchanged after dam impoundment, caused by changes in unidirectional flow dynamics driven by the altered runoff discharge (Han et al., 2018; Zhu et al., 2019). However, the morphological evolution in branches of tidal-affected braided reaches (including bifurcated estuaries) are more intricate, mainly due to the complexity of bifurcating systems and the jacking effect of tidal currents (Zhang et al., 2015; Zhu et al., 2017, 2018). Marine dynamic factors, such as waves, longshore currents, and storm surges, further complicate morphological changes in estuarine areas (Kaliraj et al., 2014; Rangoonwala et al., 2016; Shen et al., 2019).

As the largest river on the Eurasian continent and the third longest in the world, the Yangtze has accommodated the construction of more than 50,000 dams since the 1950s (Yang et al., 2011, 2015). Moreover, the Yangtze River hosts 49 major braided reaches in its middle and lower region (including the Yangtze Estuary); these reaches are classified into three main types: straight braided reaches; slightly bending braided reaches; and goose-head braided reaches (Yu, 2013). Under the impact of the dams, the intra-annual distribution of runoff discharge has flattened, whereas the total yearly runoff flux has hardly changed (Zhao et al., 2018; Zhu et al., 2017, 2018, 2019). Consequently, changes to the natural evolutionary trends of the branching channels have been generally identified in the braided reaches along the Yangtze River (Han et al., 2018; Zhu et al., 2017, 2019). Nevertheless, the braided near-estuary reach, which extends from the tidal current limit of the Yangtze River to the upper boundary-node of the Yangtze Estuary (Yu and Lu, 2005), has not yet been investigated comprehensively. Researchers have chiefly analyzed the evolutionary courses of thalwegs, cross-sections,

and flow hydrodynamics (e.g. net discharge ratios and flow velocities) in the branching channels of the near-estuary reach (Jiang et al., 2012b; Chen et al., 2012, 2016; Fan et al., 2017; Zhang and Xu, 2017), but have not considered overall variations in channel morphology and systemic relationships between erosion-deposition patterns and variations in the flow hydrodynamics. This implies that, predictions of the future evolution of branching channels in this reach (Jiang et al., 2012b; Chen et al., 2016) might be unreliable. Moreover, the law of depo-center movement in the branching channels of the near-estuary reach has not been explored. (The depo-center is defined as the location where the sediment deposition rate is a maximum.) Depo-center movement has not been considered previously for other braided reaches or river systems as well, and deserves in-depth analysis given its indicative role regarding erosion-deposition distributions in the branching channels of a braided river.

In the present study, the overall morphological evolution and the law of depo-center migration in branching channels of the near-estuary reach of the Yangtze River are investigated, based on terrain and hydrodynamic data from 1950 to 2014. The findings may be transferable to other braided reaches worldwide, and should be useful in guiding future engineering projects that are planned for the near-estuary reach of the Yangtze River.

2 Study area

The near-estuary reach of the Yangtze River is located at the distal section of the Yangtze River (Fig. 1(a)), extending from Jiangyin (the tidal current limit) to Xuliujing (the upper boundary-node of the Yangtze Estuary) (Yu and Lu, 2005). The reach is of

length ~ 90 km (Fig. 1(b)). Its main braided waterways comprise the Fujiangsha, Rugaosha, Tongzhousha, and Langshansha Waterways (Fig. 1(b)). The middle branch of the Rugaosha Waterway connects with the north branch of the Fujiangsha Waterway, whilst the Liuhaisha branch of the Rugaosha Waterway connects to the middle and south branches of the Fujiangsha Waterway (Fig. 1(b)). Similarly, the east and west branches of the Langshansha Waterway connect with the corresponding branches of the Tongzhousha Waterway (Fig. 1(b)). This braided reach is influenced by tides, with multi-year (1950-2014) average tidal ranges of 1.68 and 2.04 m at Jiangyin and Xuliujing (Fig. 1(b)) (Zhu et al., 2018). Due to the relative stability of tidal forcing at the yearly time scale (Horrevoets et al., 2004; Jiang et al., 2012a; Zhu et al., 2017), the mean annual tidal level at Xuliujing (the lower boundary of this reach, Fig. 1(b)) is almost constant (Zhu et al., 2018). By comparison, runoff discharge from Datong hydrological station (Fig. 1(a)), representing the most downstream reach (Zhao et al., 2018; Zhu et al., 2017, 2018, 2019), experiences significant intra-annual variability, exhibited by a reduced flood discharge occurrence frequency and increased middle-low discharge occurrence frequency (Zhu et al., 2017, 2018, 2019). However, the annual runoff discharge is almost constant (Zhao et al., 2018; Zhu et al., 2017, 2018, 2019), with a multi-year (1950-2014) average value of $8930 \text{ m}^3/\text{s}$ (CWRC, 2016). To achieve the national goal of a Golden Waterway, extensive channel improvements have been implemented along the near-estuary reach, including an upstream extension of the Deepwater Channel Project (Chen et al., 2012; Wu et al., 2013; Yang and Lin, 2013; Ni et al., 2014; Xu et al., 2014).

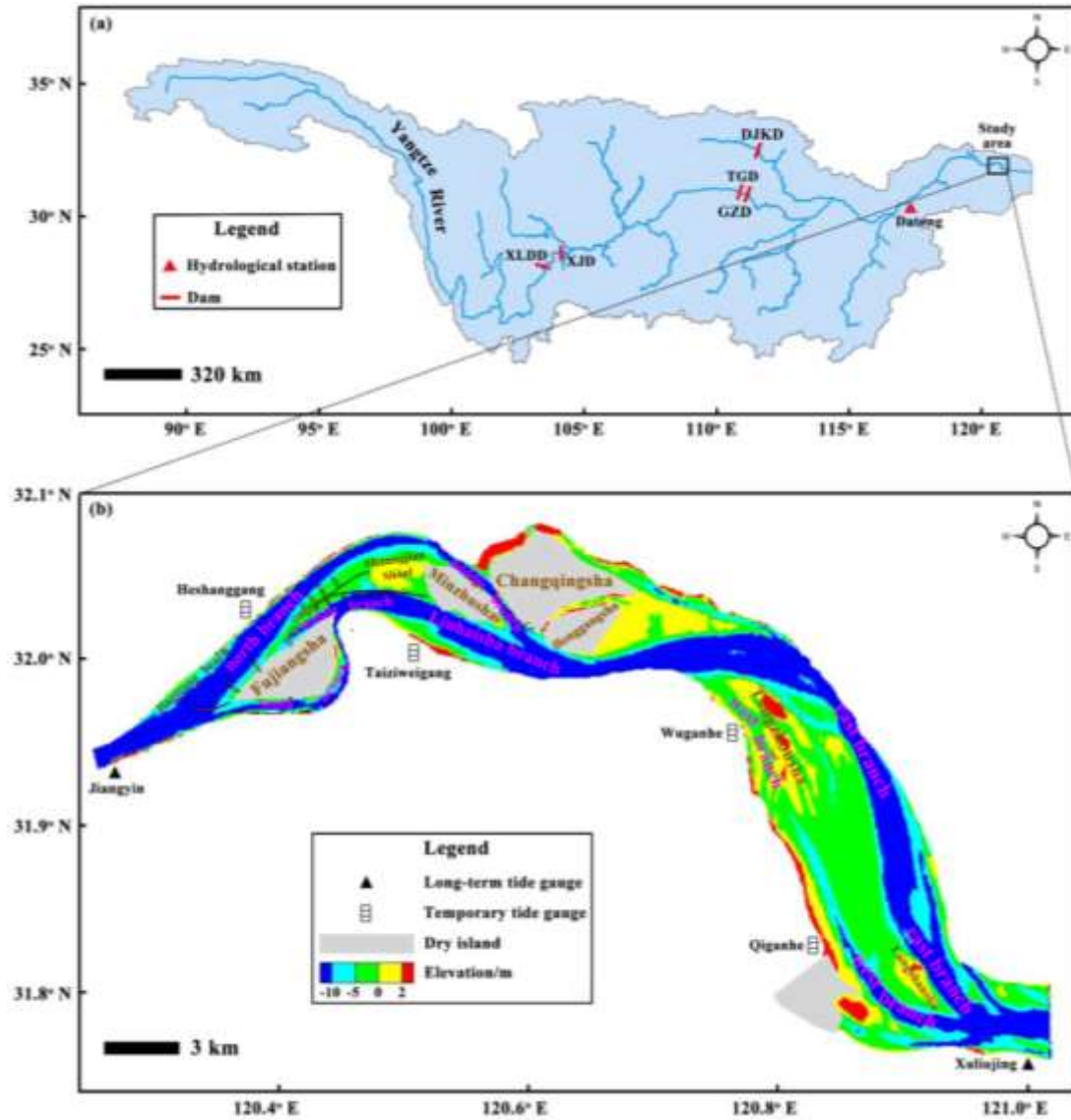


Fig. 1 The Yangtze Basin and its near-estuary reach. (a) Outline map of the Yangtze Basin indicating the locations of the Xiluodu Dam (XLDD), Xiangjia Dam (XJD), Three Gorges Dam (TGD), Gezhou Dam (GZD), Danjiangkou Dam (DJKD), Datong hydrological station, and the near-estuary reach (the study area). The years of impoundment of the dams were 2013, 2012, 2003, 1981 and 1968, respectively. (b) Bathymetry of the branched near-estuary reach, with positions of tide gauges superimposed.

3 Materials and methods

3.1 Data information

Observed daily runoff discharge time series at Datong station from 1950 to 2014, and hourly ebb tidal discharges in the branching channels and hourly ebb tidal levels at temporary tide gauges in the vicinity of the waterways from 30th August to 10th

September 2004 and from 17th January to 12th February 2005 were obtained from the Changjiang Water Resources Commission (China). Bed-elevation point data digitized from surveyed navigational charts in 2005 and 2007 were provided by the Shanghai Estuarine & Coastal Science Research Center (China); those in 2011 and 2014 were obtained from the Changjiang Waterway Bureau (China). Channel volumes below -5 m and -10 m isobaths in the two branches of the Tongzhousha Waterway were acquired from the Changjiang Waterway Bureau (China). The following data on hydrodynamics and morphology were gathered from the open literature: (1) yearly wet-season average ebb partition ratios for branching channels in 1977, 1983, 1993, 1998, 2006, and 2011; (2) minimum widths of -8 m and -10 m isobaths in the north branch of the Fujiangsha Waterway from 2005 to 2012; (3) cross-sectional profiles at the entrance of the south branch of the Fujiangsha Waterway in 1977, 1983, 1993, 1998, 2006, and 2011; and (4) cross-sectional areas of the two branches of the Rugaosha Waterway under bankfull discharge in 1977, 1983, 1993, 1998, 2006, and 2011. Table 1 summarizes the data sources.

Table 1 Data information

Type	Name	Time	Source(s)
Hydrodynamics	Daily runoff discharge series	1950-2014	Changjiang Water Resources Commission (China)
	Hourly ebb tidal discharge series in the branching channels	2004.08.30-2004.09.10, 2005.01.17-2005.02.12	Changjiang Water Resources Commission (China)
	Hourly tidal level series at temporary tide gauges in vicinity of the waterways ^{a)}	2004.08.30-2004.09.10, 2005.01.17-2005.02.12	Changjiang Water Resources Commission (China)
	Yearly wet-season	1977, 1983, 1993, 1998,	Chen et al., 2016

	average ebb partition ratios in the branching channels	2006, 2011	
	Bed-elevation point data of the whole near-estuary reach	2005, 2007, 2011, 2014	Shanghai Estuarine & Coastal Science Research Center (China) and Changjiang Waterway Bureau (China)
	Minimum widths of -8 m and -10 m isobaths in the north branch of Fujiangsha Waterway	2005-2012	Yang and Lin, 2013
Morphology	Cross-sectional profile at the entrance of the south branch of Fujiangsha Waterway	1977, 1983, 1993, 1998, 2006, 2011	Chen et al., 2012
	Cross-sectional areas of the two branches of Rugaoshan Waterway under bankfull discharge	1977, 1983, 1993, 1998, 2006, 2011	Wu et al., 2013
	Channel volumes below -5 m and -10 m isobaths in both branches of Tongzhousha Waterway	1977, 1983, 1993, 1997, 1998, 2001, 2004, 2006, 2008, 2009, 2010	Changjiang Waterway Bureau (China)

^{a)} The nearby temporary tide gauges are at Heshanggang, Taiziweigang, Wuganhe, and Qiganhe stations, as indicated on Fig. 1(b).

3.2 Processing of bed-elevation point data

Bed-elevation point data from 2005, 2007, 2011, and 2014 were projected onto Beijing 54 coordinates using ArcGIS 10.2 during digitization, with reference to 1985 national elevation benchmarks. Bed elevations and point locations had previously been determined from measurements using dual-frequency echo sounders and GPS positioning. The measurement errors for bed-elevation of ± 0.1 m and location of ± 1 m were taken to be acceptable, noting the huge scale of bed-elevation changes that can occur annually (Luan et al., 2016). The proportional scales for all the four sets of terrain

data are 1:10,000, with sample density of 10 – 122 pts/km² (i.e. spacing of 50 – 500 m between two neighboring points), and so a grid resolution of 25 m × 250 m was adopted when calculating morphological changes using Kriging interpolation.

3.3 Interpretation of depo-centers

A depo-center in a branching channel is defined as the location where the maximum depositional rate of sediment occurs. Upstream and downstream depo-center movements in branching channels are identified by interpreting changes in river-bed elevation caused by erosion and deposition in upper and lower sub-reaches of roughly the same length. Increases in depositional rate or decreases in erosional rate of the upper or lower sub-reaches indicate that the depo-centers in the corresponding channels are moving towards the sub-reaches, whereas decreases in depositional rate or increases in erosional rate of the sub-reaches indicate depo-center movements away from the sub-reaches. Fig. 2 illustrates the divisions of upper and lower sub-reaches in the branching channels of the four main braided waterways.

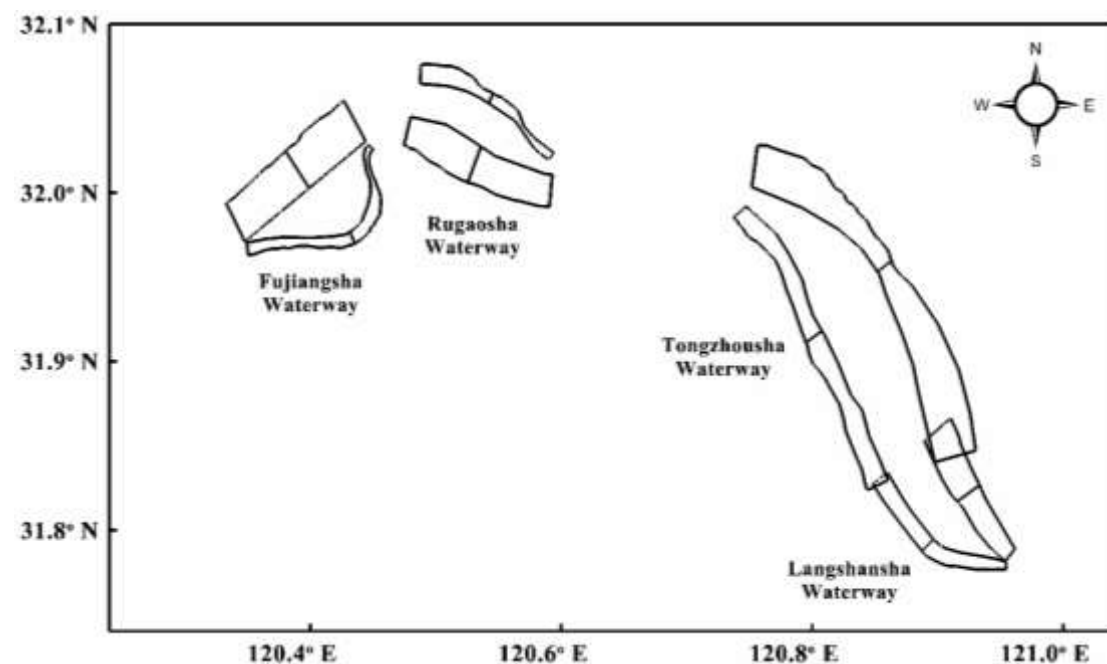


Fig. 2 Boundaries of branching channels and their upper and lower sub-reaches.

4 Results

4.1 Hydrodynamic variations

4.1.1 Runoff discharge

Fig. 3 shows that the yearly runoff discharge changed little, whereas the intra-annual distribution of runoff discharge flattened significantly, from the pre-TGD period (in which the GZD and the DJKD impounded water, Fig. 1) before the TGD became operational to the post-TGD period (in which the TGD, the XJD and the XLDD impounded water, Fig. 1) afterwards. It can be seen that the multi-year average duration days of discharges $< 10,000 \text{ m}^3/\text{s}$ and $> 50,000 \text{ m}^3/\text{s}$ decreased significantly, while those of $10,000\text{--}20,000 \text{ m}^3/\text{s}$ increased substantially.

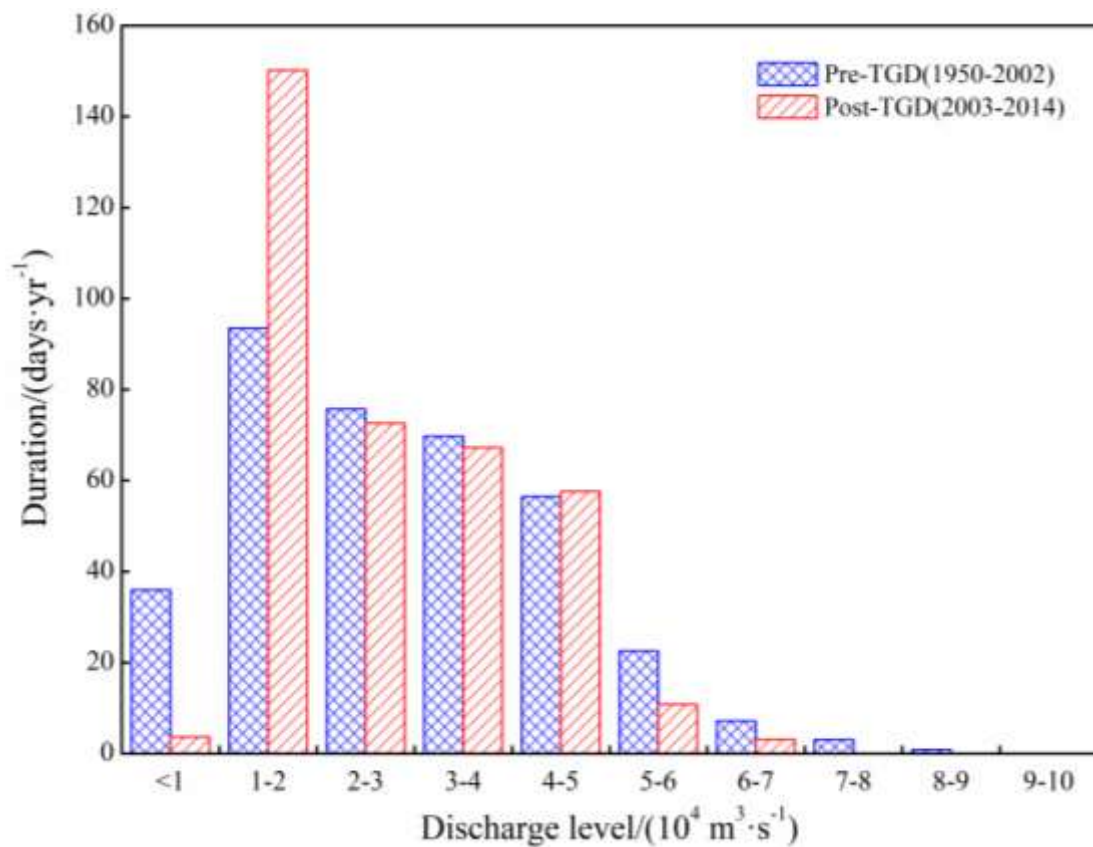


Fig. 3 Histogram of annual mean duration days for different runoff discharge levels at Datong station from 1950 to 2002 before impoundment of the TGD (and also XJD and XLDD, Fig. 1(a)) and from

2003 to 2014 after its impoundment, during which time both XLDD and XJD also commenced operation.

4.1.2 Ebb partition ratio

4.1.2.1 Yearly trends

Fig. 4 shows that the yearly wet-season average ebb partition ratios in the north region (including the north branch, middle branch, and Shuangjian shoal, Fig. 1(b)) of Fujiangsha Waterway, the Liuhaisha branch of Rugaosha Waterway, the west branch of Tongzhousha Waterway, and the west branch of Langshansha Waterway exhibited decreasing trends from 1977 to 2011, whereas the ebb partition ratios for the other branches of the four waterways presented increasing trends.

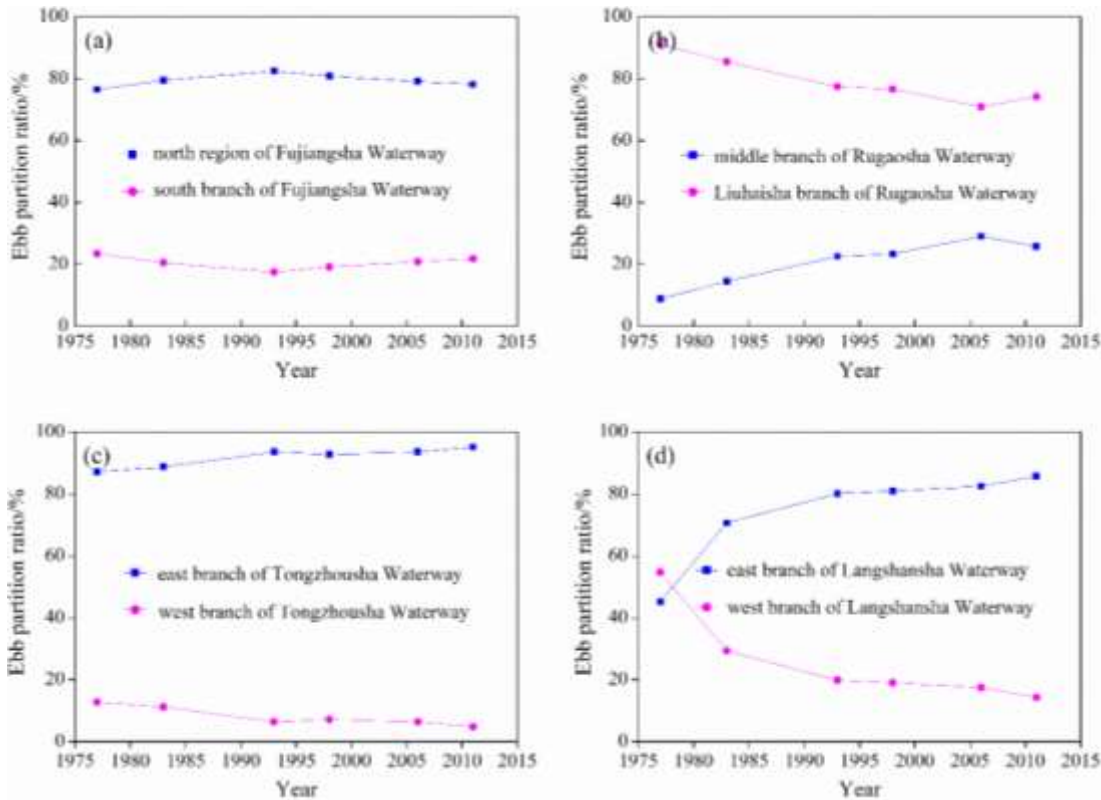


Fig. 4 Trends in annual wet-season average ebb partition ratios for branching channels of the following waterways: (a) Fujiangsha; (b) Rugaosha; (c) Tongzhousha; and (d) Langshansha.

4.1.2.2 Changes under different runoff conditions

Fig. 5 presents the variations in ebb partition ratio with tidal range obtained for the

branching channels from 30th August to 10th September 2004 and from 17th January to 12th February 2005, for runoff discharges of 36,000 m³/s and 11,000 m³/s. The tidal data were obtained using temporary tide gauges (see Fig. 1(b) for locations). For all tidal range values considered, the ebb partition ratio at a runoff discharge of 36,000 m³/s was invariably larger than that at 11,000 m³/s in the north region of Fujiangsha Waterway, the Liuhaisha branch of Rugaosha Waterway, the west branch of Tongzhousha Waterway, and the west branch of Langshansha Waterway. This implies that the higher runoff discharge caused flow to divert into these branches, with the opposite occurring in the other waterway branches.

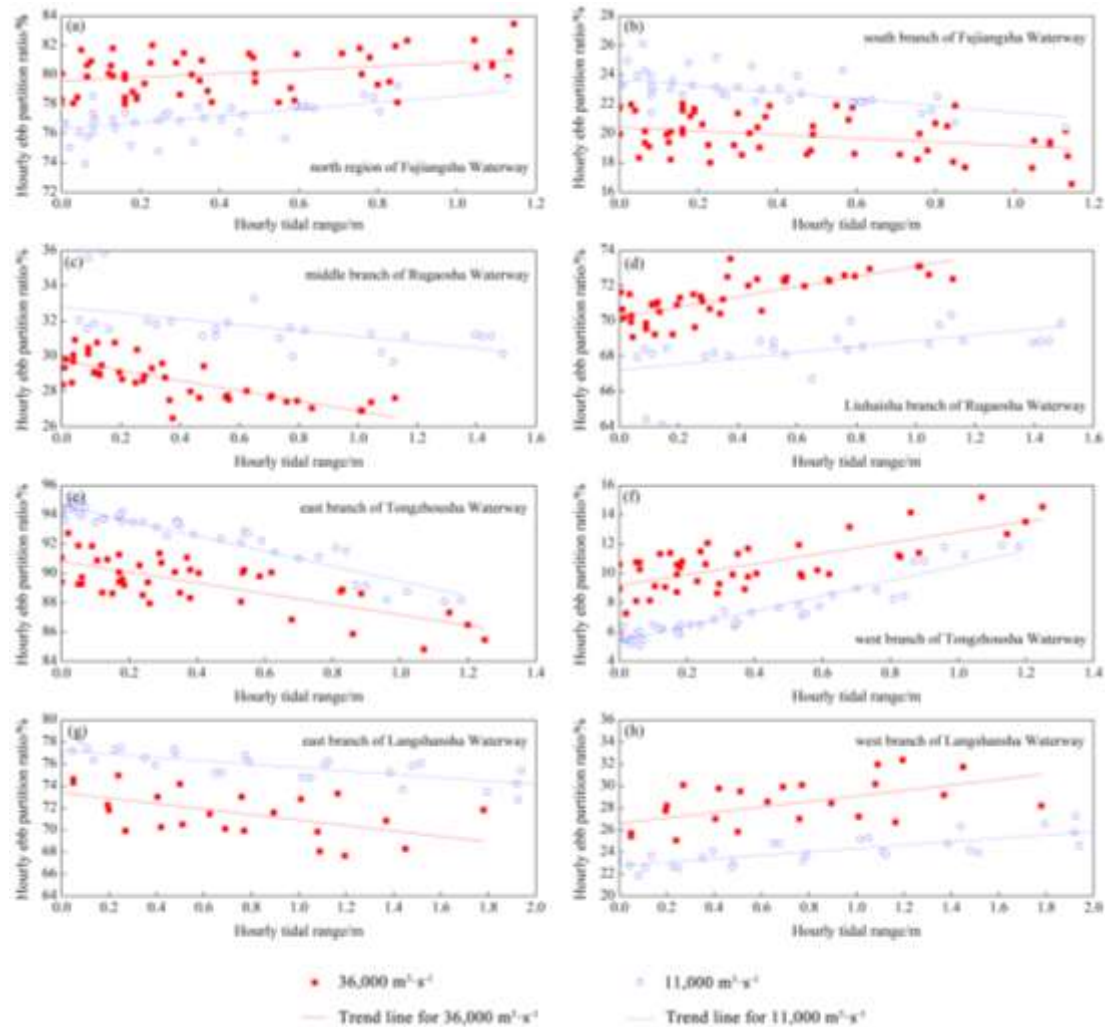


Fig. 5 Relationships between ebb partition ratio and tidal range for two runoff discharge levels in

the branching channels of the waterways: (a) north region of Fujiangsha Waterway; (b) south branch of Fujiangsha Waterway; (c) middle branch of Rugaosha Waterway; (d) Liuhaisha branch of Rugaosha Waterway; (e) east branch of Tongzhousha Waterway; (f) west branch of Tongzhousha Waterway; (g) east branch of Langshansha Waterway; and (h) west branch of Langshansha Waterway. Each hourly tidal range value was determined by subtracting the average of preceding and succeeding low tidal levels from the hourly tidal level.

4.2 Morphological variations

4.2.1 Whole channel

4.2.1.1 Yearly trends

Both the annual time series of minimum widths of the -8 m and -10 m isobaths in the north branch of the Fujiangsha Waterway present decreasing temporal trends (Fig. 6(a)), indicating that the north branch has been progressively shrinking. Given that the north branch is the main channel at the north of Fujiangsha Island (Fig. 1(b)), this shrinkage implies that the northern region (including the north branch, middle branch, and Shuangjian shoal) of the Fujiangsha Waterway has been experiencing morphological decline. By contrast, the deep channel of the cross-section at the entrance of the south branch of Fujiangsha Waterway underwent significant erosion from 1977 to 2011 (Fig. 6(b)), suggesting the morphology of the south branch was undergoing rapid development. The cross-sectional areas of the middle branch and the Liuhaisha branch of Rugaosha Waterway presented increasing and decreasing trends under bankfull discharge (Figs. 6(c-d)), implying the middle branch and Liuhaisha branch were experiencing developing and declining morphological trends respectively. Figs. 6(e-f) show that the channel volume below the -10 m isobath in the east branch of the Tongzhousha Waterway has been presenting an increasing trend, whereas that below the -5 m and -10 m isobaths in the west branch of the Tongzhousha Waterway has a

decreasing trend, indicating development and decline of the east and west branches respectively.

It should be noted that field observations by Chen et al. (2016) have shown that the east and west branches of the Langshansha Waterway have exhibited developing and declining trends.

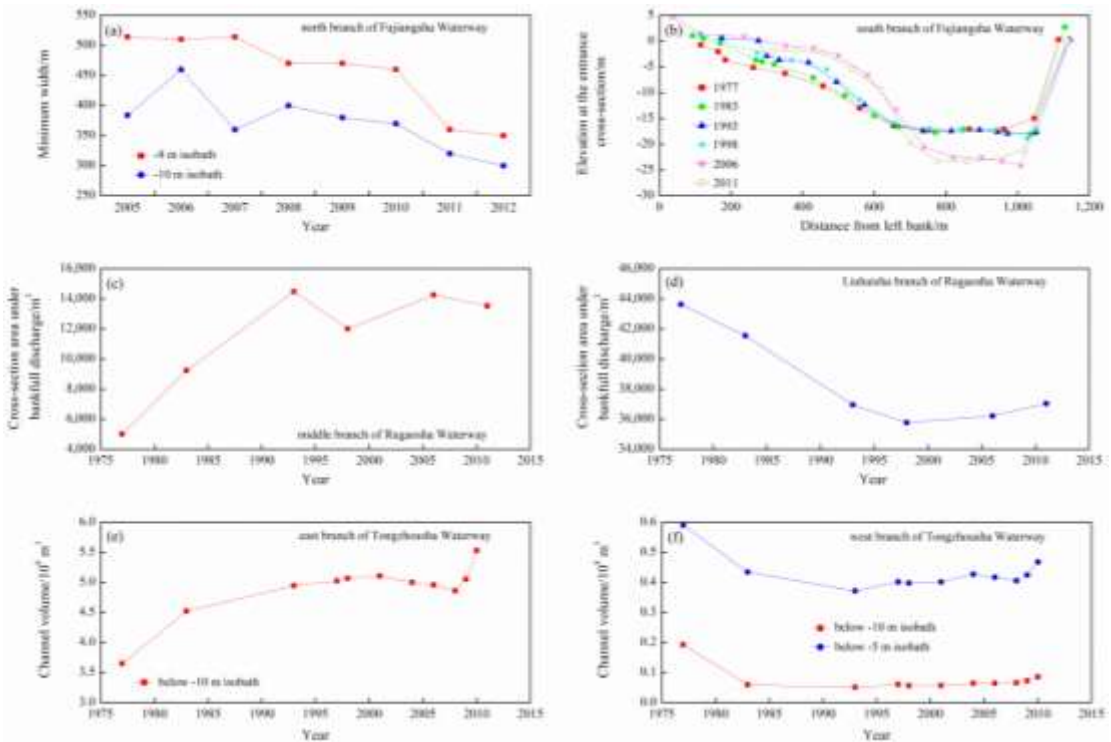


Fig. 6 Evolution of the branching channels of the waterways: (a) annual values of minimum widths of -8 m and -10 m isobaths in the north branch of Fujiangsha Waterway; (b) evolution of the cross-section at the entrance of the south branch of Fujiangsha Waterway; (c) annual time series of the cross-sectional area under bankfull discharge of the middle branch of Rugaoshan Waterway; (d) evolution of the cross-sectional area under bankfull discharge of Liuhaisha branch of Rugaoshan Waterway; (e) temporal behavior of channel volume below -10 m isobath of the east branch of Tongzhousha Waterway; and (f) temporal behavior of channel volume below -10 m and -5 m isobaths of the west branch of Tongzhousha Waterway.

4.2.1.2 Changes under different runoff conditions

Table 2 lists erosion-deposition rates in the branching channels and the corresponding duration days of relevant runoff discharges during 2005-2007, 2007-2011, and 2011-2014. Fig. 7 displays plan distributions of erosion-deposition rates for

the whole near-estuary reach in 2005, 2007, 2011, and 2014. Of these periods, 2005-2007 was the driest, being associated with the least duration days of flood discharges ($> 50,000 \text{ m}^3/\text{s}$ and $> 60,000 \text{ m}^3/\text{s}$) and the most duration days of low and middle-low discharges ($< 10,000 \text{ m}^3/\text{s}$ and $10,000 - 20,000 \text{ m}^3/\text{s}$) (Table 2). This is because the 2005-2007 period contained an extreme dry year event that affected the Yangtze Basin in 2006 (Zhu et al., 2018); during this event no discharge exceeded $40,000 \text{ m}^3/\text{s}$, and the duration days of low and middle-low discharges were at 7 days and 185 days. The 2007-2011 period was wettest, with the largest number of duration days for flood discharges (especially $> 60,000 \text{ m}^3/\text{s}$) and lower numbers of duration days for low and middle-low discharges than in 2005-2007 (Table 2). The 2007-2011 period included the flood year of 2010 (Zhu et al., 2018), the only year during which the discharge exceeded $60,000 \text{ m}^3/\text{s}$ in the total period from 2005 to 2014. In 2010, the duration of the $> 60,000 \text{ m}^3/\text{s}$ discharge lasted 36 days. The runoff intensity in 2011-2014 was between that in the foregoing two periods (Table 2).

The entire northern region of Fijiangsha Waterway (including the north branch, middle branch, and Shuangjian shoal) experienced deposition during 2005-2007, severe erosion during 2007-2011, and slight erosion during 2011-2014 (Table 2), indicating that low and high values of runoff intensity promoted deposition and erosion respectively. This erosion-deposition behavior in the north region is also confirmed by changes in the deep channel area (see Fig. 7), which shrank in the period from 2005 to 2007 (Figs. 7(a-b)) before experiencing significant growth from 2007 to 2011 (Figs. 7(b-c)) and from 2011 to 2014 (Figs. 7(c-d)). Erosion occurred in the south branch

during all three periods, with a much larger erosional rate during 2005-2007 than 2011-2014 (Table 2). Even though severe erosion occurred in the south branch during 2007-2011 when the largest number of flood discharge duration days were experienced, the rate of erosion was smaller than in the north region (Table 2; Figs. 7(b-c)). This implies that the north region and south branch underwent roughly the reverse erosion-deposition behavior under runoff changes.

In accordance with changes in runoff intensity, the Liuhaisha branch of Rugaosha Waterway experienced deposition during 2005-2007, significant erosion during 2007-2011, and less significant erosion during 2011-2014 (Table 2). This erosion-deposition behavior was linked to changes in the deep channel area (Fig. 7) which witnessed obvious shrinkage from 2005 to 2007 (Figs. 7(a-b)) and significant growth from 2007 to 2011 (Figs. 7(b-c)) and 2011 to 2014 (Figs. 7(c-d)). The middle branch of Rugaosha Waterway exhibited a similar erosion-deposition pattern to that of the Liuhaisha branch (Table 2), influenced by the flood-tide-driven sediment supply from the lower two braided waterways during the dry period of 2005-2007 (Zhu et al., 2018) and engineering projects implemented in the vicinity (Fig. 1(b); Chen et al., 2012; Wu et al., 2013).

The two branches of Tongzhousha Waterway did not exhibit opposite erosion-deposition patterns under runoff change (Table 2); this was perhaps because the gradual decline of the west branch in recent years (Ni et al., 2014) caused the Tongzhousha Waterway effectively to become a single river channel dominated by the east branch. In this case, the discharge, regardless of runoff intensity, passed mainly through the east

branch, leading to erosion or deposition depending on the flow speed within the branch (Table 2). Meanwhile, regulation projects implemented along the Tongzhousha Waterway also impacted on the erosion-deposition pattern (Ni et al., 2014). Even so, the low runoff intensity during 2005-2007 promoted shrinkage of the west branch and shortened the deep channel of the west branch (Figs. 7(a-b)), whereas the high runoff intensities during 2007-2011 and 2011-2014 facilitated development of the west branch, lengthening its deep channel (Figs. 7(b-c) and 7(c-d)). The upper and lower deep channels became connected within the west branch from 2011 to 2014 (Figs. 7(c-d)).

Depositional rates in the east branch of Langshansha Waterway were smallest during 2005-2007 and largest during 2007-2011 (Table 2), indicating that low and high runoff intensities respectively facilitated the development and decline of the east branch. As shown in Fig. 7, the deep channel area in the east branch experienced obvious growth from 2005 to 2007, and altered from a bifurcating to a single channel pattern as its width increased (Figs. 7(a-b)). However, from 2007 to 2011 and 2011 to 2014 the deep channel area re-established a bifurcated pattern, with decreased width (Figs. 7(b-c) and 7(c-d)). The west branch underwent an almost opposite erosion-deposition pattern, with deposition during 2005-2007 and 2011-2014, and erosion during 2007-2011 (Table 2); this implied that low runoff intensity promoted shrinkage of the west branch whereas high runoff intensity promoted growth. Meanwhile, the deep channel of the west branch shortened during 2005-2007 (Figs. 7(a-b)) and lengthened during 2007-2011 (Figs. 7(b-c)) and 2011-2014 (Figs. 7(c-d)).

In summary, low runoff intensity generally promoted development of the south

334 branch of Fujiangsha Waterway, the middle branch of Rugaosha Waterway, the east
335 branch of Tongzhousha Waterway, and the east branch of Langshansha Waterway, while
336 usually facilitating morphodynamic decline of the other branches of the braided
337 waterways. High runoff intensity produced essentially the opposite effect.

338 **Table 2** Erosional/depositional rates (deposition positive-valued, and erosion negative-valued) of branching channels at the near-estuary reach of the Yangtze River
339 over different periods, and corresponding multi-year average duration days of different runoff discharges at Datong station

Waterway	Branching channel	Period	Erosional/Depositional rate/(m·yr ⁻¹) ^{a)}	Annual mean duration days of runoff discharge at Datong station/(days·yr ⁻¹) ^{b)}			
				<10,000 m ³ ·s ⁻¹	10,000-20,000 m ³ ·s ⁻¹	>50,000 m ³ ·s ⁻¹	>60,000 m ³ ·s ⁻¹
Fujiangsha	north region	2005-2007	0.650	4	170	10	0
		2007-2011	-0.458	0	168	14	7
		2011-2014	-0.186	0	156	14	0
	south branch	2005-2007	-0.147	4	170	10	0
		2007-2011	-0.314	0	168	14	7
		2011-2014	-0.020	0	156	14	0
Rugaosha	middle branch	2005-2007	0.348	4	170	10	0
		2007-2011	-0.603	0	168	14	7
		2011-2014	-0.123	0	156	14	0
	Liuhaisa branch	2005-2007	0.902	4	170	10	0
		2007-2011	-0.224	0	168	14	7
		2011-2014	-0.156	0	156	14	0
Tongzhousha	east branch	2005-2007	0.310	4	170	10	0

Langshansha	west branch	2007-2011	-0.147	0	168	14	7
		2011-2014	0.024	0	156	14	0
		2005-2007	-0.095	4	170	10	0
		2007-2011	-0.018	0	168	14	7
		2011-2014	-0.678	0	156	14	0
		2005-2007	0.005	4	170	10	0
	east branch	2007-2011	0.711	0	168	14	7
		2011-2014	0.201	0	156	14	0
		2005-2007	0.458	4	170	10	0
	west branch	2007-2011	-0.229	0	168	14	7
		2011-2014	0.767	0	156	14	0

^{a)} Fig. 2 shows boundaries of the branching channels.

^{b)} < 10,000 m³/s, 10,000-20,000 m³/s and > 50,000 m³/s are the discharge levels experiencing obvious changes in duration days over different periods (Fig. 3), whereas 60,000 m³/s approximates the bed-forming discharge in the near-estuary reach of the Yangtze River (Yun, 2004).

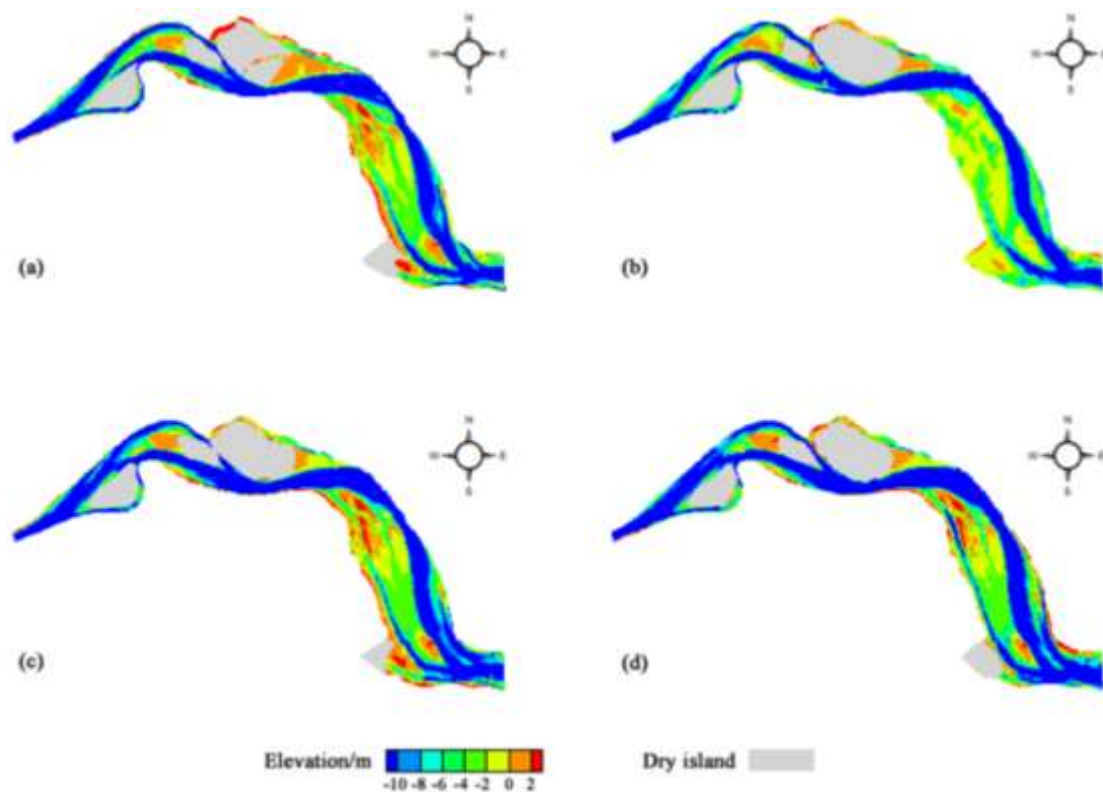


Fig.7 Plan distributions of river bed elevation at the near-estuary reach of the Yangtze River in (a) 2005, (b) 2007, (c) 2011, and (d) 2014.

4.2.2 Depo-center movement

The data listed in Table 3 indicate that depo-centers in the north region of Fujiangsha Waterway, the Liuhaisha branch of Rugaosha Waterway, the west branch of Tongzhousha Waterway, and the west branch of Langshansha Waterway moved upstream when the runoff intensity declined, and moved downstream when runoff intensity rose. The situation for the other branches of the waterways was quite the opposite. The details are as follows:

In the north region of the Fujiangsha Waterway, the depositional rate in the upper sub-reach was larger than in the lower sub-reach during 2005-2007 (with low runoff intensity) (Table 3), indicating that the depo-center of this region was located in the upper sub-reach. However, both sub-reaches experienced erosion during 2007-2011 and 2011-2014 (with higher runoff intensities) (Table 3), implying that the depo-center

358 moved into the channel downstream of this region. Moreover, because runoff intensity
359 during 2007-2011 was higher than during 2011-2014, the erosion rates of the two sub-
360 reaches during 2007-2011 were larger than during 2011-2014, and the erosion rate in
361 the upper sub-reach was larger than in the lower sub-reach during 2007-2011 (Table 3).
362 This suggested that the depo-center moved further downstream during 2007-2011 than
363 2011-2014. Due to the likely impacts of regulation projects in the Fujiangsha Waterway
364 (Fig. 1(b); Xu et al., 2014), the depo-center in the south branch did not exhibit the
365 reverse behavior (Table 3).

366 The depositional rate in the lower sub-reach of the middle branch of Rugaoshan
367 Waterway was larger than in its upper sub-reach during 2005-2007 (Table 3), indicating
368 that the depo-center was located in the lower sub-reach. During 2007-2011, both sub-
369 reaches underwent erosion (Table 3), implying that the depo-center was located in the
370 channel downstream of the middle branch. However, the erosional rate in the upper
371 sub-reach was smaller than in the lower sub-reach during 2007-2011 (Table 3). This
372 suggests that the downstream movement of the depo-center was eased by an upstream
373 transport of sediment (eroded from the lower sub-reach during flood-tide) into the upper
374 sub-reach during this flood period. The runoff intensity from 2011 to 2014 had a value
375 between those during 2005-2007 and 2007-2011, and so the position of the depo-center
376 (reflected by the erosion-deposition rates of the two sub-reaches, Table 3) occupied an
377 intermediate location. The depo-center in the Liuhaisha branch exhibited almost the
378 opposite behavior. Both sub-reaches of the Liuhaisha branch experienced deposition
379 during 2005-2007 and erosion during 2007-2011 and 2011-2014 (Table 3), suggesting

that the depo-center was located in the Liuhaisha branch during the former period but in the channel downstream of the Liuhaisha branch during the latter two periods. In short, the depo-center migrated downstream from 2005 to 2014. Meanwhile, the decrease in erosional rate of the upper sub-reach was larger than that of the lower sub-reach from 2007-2011 to 2011-2014 as runoff intensity fell (Table 3), indicating upstream migration of the depo-center.

Both sub-reaches of the east branch of the Tongzhousha Waterway experienced erosion during 2007-2011 (Table 3), corresponding to the depo-center being located in the channel downstream of the east branch. However, the erosional rate in the upper sub-reach was smaller than in the lower sub-reach (Table 3). This meant that erosion in the upper sub-reach was relieved by upstream transport of sediment (eroded from the lower sub-reach by the flood-tide) into the upper sub-reach. During 2005-2007 and 2011-2014, the upper and lower sub-reaches underwent erosion and deposition (Table 3), implying that the depo-center was located in the lower sub-reach. In the west branch, the upper and lower sub-reaches respectively experienced erosion and deposition during 2005-2007 (Table 3), indicating that the depo-center was located in the lower sub-reach. However, both sub-reaches experienced erosion during 2011-2014, with the erosional rate of the upper sub-reach increasing significantly (Table 3), as the depo-center moved into the channel downstream of the west branch.

During 2005-2007, the upper and lower sub-reaches of the east branch of the Langshansha Waterway experienced erosion and deposition, respectively (Table 3), with the depo-center accordingly located in the lower sub-reach. During 2007-2011 and

402 2011-2014, the upper sub-reach accreted sediment, whilst the lower sub-reach
403 underwent deposition (during 2007-2011) followed by erosion (during 2011-2014)
404 (Table 3), meaning that the depo-center moved upstream, even entering the upper sub-
405 reach. The upper and lower sub-reaches of the west branch experienced deposition and
406 erosion respectively during 2005-2007 and 2011-2014 (Table 3) when the depo-center
407 was located in the upper sub-reach. However, the upper and lower sub-reach underwent
408 erosion and deposition respectively during 2007-2011 (Table 3), as the depo-center
409 migrated downstream in the lower sub-reach during this flood period.

410 **Table 3** Erosional/depositional rates (deposition positive-valued, and erosion negative-valued) for upper and lower sub-reaches of the branching channels at the near-
411 estuary reach of the Yangtze River over different periods and corresponding multi-year average duration days of different runoff discharges at Datong station

Waterway	Branching channel	Period	Erosional/Depositional rate of upper sub-reach/(m·yr ⁻¹) ^{a)}	Erosional/Depositional rate of lower sub-reach/(m·yr ⁻¹) ^{a)}	Annual mean duration days of runoff discharges at Datong station/(days·yr ⁻¹) ^{b)}			
					<10,000	10,000-20,000	>50,000	>60,000
					m ³ ·s ⁻¹	m ³ ·s ⁻¹	m ³ ·s ⁻¹	m ³ ·s ⁻¹
Fujiangsha	north region	2005-2007	1.083	0.212	4	170	10	0
		2007-2011	-0.553	-0.359	0	168	14	7
		2011-2014	-0.170	-0.211	0	156	14	0
	south branch	2005-2007	0.802	-1.331	4	170	10	0
		2007-2011	-0.481	-0.087	0	168	14	7
		2011-2014	0.089	-0.131	0	156	14	0
Rugaosha	middle branch	2005-2007	0.091	0.820	4	170	10	0
		2007-2011	-0.383	-1.023	0	168	14	7
		2011-2014	-0.543	0.635	0	156	14	0
	Liuhaisha branch	2005-2007	0.487	1.437	4	170	10	0
		2007-2011	-0.203	-0.308	0	168	14	7
		2011-2014	-0.038	-0.265	0	156	14	0
Tongzhousha	east branch	2005-2007	-0.229	0.708	4	170	10	0
		2007-	-0.113	-0.172	0	168	14	7

Langshansha	west branch	2011- 2014	-0.668	0.535	0	156	14	0
		2005- 2007	-0.260	0.036	4	170	10	0
		2007- 2011	0.324	-0.293	0	168	14	7
		2011- 2014	-1.444	-0.063	0	156	14	0
	east branch	2005- 2007	-0.579	0.778	4	170	10	0
		2007- 2011	0.507	0.982	0	168	14	7
		2011- 2014	0.588	-0.311	0	156	14	0
	west branch	2005- 2007	0.938	-0.122	4	170	10	0
		2007- 2011	-0.433	0.017	0	168	14	7
		2011- 2014	1.977	-0.681	0	156	14	0

^{a)} Fig. 2 shows boundaries of upper and lower sub-reaches of the branching channels.

^{b)} < 10,000 m³/s, 10,000-20,000 m³/s and > 50,000 m³/s are the discharge levels experiencing obvious changes in duration days over periods (Fig. 3), whereas 60,000 m³/s approximates the bed-forming discharge in the near-estuary reach of the Yangtze River (Yun, 2004).

5 Discussion

5.1 Linkage-mode between channel erosion-deposition and depo-center movement

Through the foregoing analysis, a linkage-mode can be identified between the erosion-deposition patterns of branching channels and their depo-center movements. That is, as a channel experiences erosion/deposition, its depo-center tends to move downstream/upstream. In the north part of Fujiangsha Waterway, the Liuhaisha branch of Rugaosha Waterway, the west branch of Tongzhousha Waterway, and the west branch of Langshansha Waterway, erosion and concomitant downstream depo-center migration occur as runoff intensity increases, whereas deposition and accompanying upstream depo-center migration occur as runoff intensity falls (Table 2; Fig. 7; Table 3). In other branches of the waterways, the two cases of erosion-deposition behavior and concomitant depo-center migration occur as runoff intensity falls and rises, respectively (Table 2; Fig. 7; Table 3).

5.2 Mechanism behind the linkage-mode

Fig. 5 indicates that there is a robust relationship between ebb partition ratio and runoff discharge for a branching channel in the near-estuary reach, given that the morphological changes in the river bed are small, owing to the short timespan from the wet period (30th August to 10th September 2004) to the dry period (17th January to 12th February 2005), and because runoff intensity was weak during this water-recession timespan. The relationships in Fig. 5 are driven by the geographic features of the near-estuary reach. Several raised nodes (formed by mountains) exist along the south bank at the entrance of Fujiangsha Waterway (Chen et al., 1988). These nodes tend to drive

the ebb tidal current into the north region of Fujiangsha Waterway, with this effect strengthening as runoff intensity rises (Chen et al., 1988). Hence, a high runoff discharge corresponds to a high value of ebb partition ratio in the north region and a low value of ebb partition ratio in the south branch, with the reverse occurring for a low runoff discharge (Figs. 5(a-b)). The Liuhaisha branch of Rugaosha Waterway is much wider than the middle branch of Rugaosha Waterway and connects with the north region of Fujiangsha Waterway (Fig. 1(b)). Hence, a high runoff discharge also facilitates diversion of the ebb tidal current into the Liuhaisha branch while restraining diversion of the ebb tidal current into the middle branch (Figs. 5(c-d); Chen et al., 2012). Given that the cross-section and water depth of the east branch of Tongzhousha Waterway are much larger than those of the west branch (Fig. 1(b)), the ebb tidal current tends to flow into the east branch when the runoff discharge is low, which increases the ebb partition ratio in the east branch and decreases the ebb partition ratio in the west branch (Figs. 5(e-f)). Conversely, the tidal level rises as runoff discharge increases, causing part of the ebb tidal current to divert into the west branch (Chen et al., 2012), leading to the ebb partition ratio exhibiting opposite behavior in the two branches (Figs. 5(e-f)). Given that the two branches of Langshansha Waterway connect directly with those of Tongzhousha Waterway (Fig. 1(b)), the relationships between ebb partition ratio and runoff discharge of the branches are similar to those for the Tongzhousha Waterway (Figs. 5(g-h)).

In the near-estuary reach, the ebb tidal flow consists of runoff discharge and the flood tidal current, both of which are relatively stable at the yearly time scale (Zhu et

al., 2017, 2018). Consequently, the yearly ebb tidal flow is also stable, implying that ebb partition ratios in the branching channels determine the allocation of ebb tidal amplitudes among these channels. Existing theory has established that the ebb tidal force dominates channel evolution in tide-affected reaches (Dou, 1964). Hence, the ebb partition ratio is responsible for morphological change in a branching channel. During a dry period with low runoff intensity (e.g. 2005-2007), the values of ebb partition ratio (i.e. ebb tidal force) for the south branch of Fujiangsha Waterway, the middle branch of Rugaosha Waterway, the east branch of Tongzhousha Waterway, and the east branch of Langshansha Waterway were large (Figs. 5(b, c, e, g)). Hence, downstream transport of sediment tended to occur in these channels, resulting in erosion or reduced deposition in the channels (Table 2); meanwhile, the channel depo-centers were pushed downstream by the strong ebb tidal current (Table 3). Conversely, the values of ebb partition ratio for other waterway branches were small (Figs. 5(a, d, f, h)), which promoted the relative strength of the flood tide in these channels, driving upstream sediment transport from downstream reaches into the channels, leading to deposition or reduced erosion (Table 2); simultaneously, the channel depo-centers were pushed upstream by the strong flood tidal current (Table 3). During flood periods of high runoff intensity (e.g. 2007-2011 and 2011-2014), the opposite occurred (Fig. 5; Table 2; Table 3).

5.3 Trends in channel erosion-deposition and depo-center movement

The presence of dams caused decreases in duration days of discharges exceeding 50,000 m³/s and 60,000 m³/s and increases in duration days of discharges in the range

10,000—20,000 m³/s (Fig. 3). This resulted in decreasing trends in ebb partition ratios for the north region of Fujiangsha Waterway, the Liuhaisha branch of Rugaosh Waterway, the west branch of Tongzhousha Waterway, and the west branch of Langshansha Waterway, and increasing trends for the other waterway branches (Fig. 4). Accordingly, a branching channel with decreasing ebb partition ratio presented a declining trend, and vice versa (Fig. 6; Chen et al., 2016). Meanwhile, depo-centers in declining branches tended to migrate upstream and become located in the upper sub-reaches, whereas those in developing branches tended to move downstream into the lower sub-reaches, as demonstrated for recent channel-regulation projects (Wu et al., 2013; Yang and Lin, 2013; Ni et al., 2014).

At the time of writing, a cascade of large dams is being constructed along the upper Yangtze, which will continue to flatten the intra-annual distribution of runoff discharge (Duan et al., 2016). In addition, the future change in climate will help promote this kind of runoff flattening (Cao et al., 2011; Sun et al., 2013; Zeng et al., 2013; Chai et al., 2019). Consequently, recent trends in ebb partition ratios, patterns of channel erosion-deposition, and depo-center movements in the near-estuary reach of the Yangtze are likely to persist well into the future.

6 Conclusions

The north region of Fujiangsha Waterway, the Liuhaisha branch of Rugaosh Waterway, the west branch of Tongzhousha Waterway, and the west branch of Langshansha Waterway in the near-estuary reach of the Yangtze River tend to experience increased deposition or reduced erosion in periods of low runoff intensity,

and vice versa. The depo-centers in these channels have been found to move upstream and downstream under low and high runoff intensity scenarios. Meanwhile, the other waterway branches in the near-estuary reach experience opposite trends in erosion-deposition pattern and depo-center movement with varying runoff intensity.

The mechanism behind the foregoing morphological changes relates to variations in ebb partition ratio in the branching channels as the flow hydrodynamics alters, owing partly to geographic features (raised nodes and connections among the branches) of the near-estuary reach. As runoff discharge rose, the ebb partition ratios in the north region of Fujiangsha Waterway, the Liuhaisha branch of Rugaoshan Waterway, the west branch of Tongzhousha Waterway, and the west branch of Langshansha Waterway increased. Thus, sediment in these branching channels tended to be transported into downstream reaches by the ebb tidal current, resulting in erosion or reduced deposition, with the depo-centers pushed downstream. Ebb partition ratios in the other waterway branches decreased, with sediment in downstream reaches transported into the branches by the relatively stronger flood tidal current, leading to deposition or less erosion in the branches, and causing the depo-centers to migrate upstream. As runoff discharge fell, the opposite occurred.

The runoff-flattening effect of dams in Yangtze Basin has greatly decreased the duration days of flood discharges exceeding 50,000 m³/s and 60,000 m³/s, and increased those of the middle-low discharge between 10,000 and 20,000 m³/s. This in turn significantly reduced the values of ebb partition ratio in the north region of Fujiangsha Waterway, the Liuhaisha branch of Rugaoshan Waterway, the west branch of

Tongzhousha Waterway, and the west branch of Langshansha Waterway. Therefore, these branching channels have presented declining morphological trends, with their depo-centers tending to move upstream, becoming located in the upper sub-reaches. Dam-induced runoff flattening has enhanced ebb partition ratios in the other waterway branches, promoting morphological development and downstream migration of depo-centers into the lower sub-reaches of the branches. As a cascade of large dams continues to be constructed along the upper Yangtze and climate change is ongoing, current overall trends in the evolution of branching channels and migration of depo-centers are likely to be maintained into the future.

Although the current study has mainly focused on a local tide-affected braided reach of the Yangtze River, it may be instructive for other braided rivers experiencing similar hydrodynamic processes, because of its representativeness in investigating the morphological evolution in intermediate zones between the fluvial and the estuarine areas. A numerical model, which gives a full consideration of water, sediment and engineering projects, will be set up in the next step to quantify the morphological evolution of this reach.

Acknowledgements This research was supported by open funding of the Key Laboratory of Water-Sediment Sciences and Water Disaster Prevention of Hunan Province (No. 2019SS06), and the National Key Research and Development Program of China (No. 2018YFC0407201 and No. 2016YFC0402306).

Reference

Alcayaga H, Palma S, Caamano D, Mao L, Soto-Alvarez M (2019). Detecting and quantifying

547 hydromorphology changes in a Chilean river after 50 years of dam operation. *Journal of South*
548 *American Earth Sciences*, 93: 253-266

549 Cao L J, Zhang Y, Shi Y (2011). Climate change effect on hydrological processes over the Yangtze
550 River basin. *Quaternary International*, 244(2): 202-210

551 Chai Y F, Li Y T, Yang Y P, Zhu B Y, Li S X, Xu C, Liu C C (2019). Influence of climate variability
552 and reservoir operation on streamflow in the Yangtze River. *Scientific Reports*, 9: 5060

553 Changjiang Water Resources Commission (CWRC) (2016). *Changjiang River Sediment Bulletin*.
554 Wuhan: Changjiang Press (in Chinese)

555 Chen J Y, Shen H T, Yun C X, eds (1988). *Processes of Dynamics and Geomorphology of the*
556 *Changjiang Estuary*. Shanghai: Shanghai Scientific & Technical Publishers (in Chinese)

557 Chen Y P, Jiang N L, Zhang C K (2012). Riverbed evolution of upper part of Yangtze Estuary and
558 its response to the hydrodynamic changes at upstream. In: *Proceedings of the 33rd International*
559 *Conference on Coastal Engineering*. Reston: ASCE Press, 1-6

560 Chen Y P, Li J X, Wu Z G, Pan S Q (2016). Dynamic analysis of riverbed evolution: Chengtong
561 Reach of Yangtze Estuary. *Journal of Coastal Research*, 75: 203-207

562 Dai W H, Ding W (2019). Hydrodynamic improvement of a goose-head pattern braided reach in
563 lower Yangtze River. *Journal of Hydrodynamics*, 31(3): 614-621

564 Dou G R (1964). The bed form of the alluvial streams and the tidal delta. *SHUILI XUEBAO*, 1964:
565 1-13 (in Chinese)

566 Duan W X, Guo S L, Wang J, Liu D D (2016). Impact of cascaded reservoirs group on flow regime
567 in the middle and lower reaches of the Yangtze River. *Water*, 8(6): 218

568 Fan Y Y, Li Y T, Yang Y P, Huang L B (2017). Vertical velocity structure distribution in the Sansha

569 area of the Yangtze Estuary, China. *Journal of Marine Science and Technology*, 22(2): 327-334

570 Graf W L (2006). Downstream hydrologic and geomorphic effects of large dams on American rivers.

571 *Geomorphology*, 79(3-4): 336-360

572 Han J Q, Zhang W, Yuan J, Fan Y Y (2018). Channel evolution under changing hydrological regimes

573 in anabranching reaches downstream of the Three Gorges Dam. *Frontiers of Earth Science*,

574 12(3): 640-648

575 Horrevoets A C, Savenije H H G, Schuurman J N, Graas S (2004). The, influence of river discharge

576 on tidal damping in alluvial estuaries. *Journal of Hydrology*, 294(4): 213-228

577 Jain V, Sinha R (2004). Fluvial dynamics of an anabranching river system in Himalayan foreland

578 basin, Baghmata river, north Bihar plains, India. *Geomorphology*, 60(1-2): 147-170

579 Jansen J D, Nanson G C (2010). Functional relationships between vegetation, channel morphology,

580 and flow efficiency in an alluvial (anabranching) river. *Journal of Geophysical Research – Earth*

581 *Surface*, 115: F04030

582 Jiang C J, Li J F, de Swart H E (2012a). Effects of navigational works on morphological changes in

583 the bar area of the Yangtze Estuary. *Geomorphology*, 139: 205-219

584 Jiang N L, Chen Y P, Zhang C K (2012b). Channel evolution of Chengtong reach at Yangtze Estuary.

585 In: *Proceedings of the 22nd (2012) International Offshore and Polar Engineering Conference*.

586 San Francisco: ISOPE Press, 1382-1386

587 Kaliraj S, Chandrasekar N, Magesh N S (2014). Impacts of wave energy and littoral currents on

588 shoreline erosion/accretion along the south-west coast of Kanyakumari, Tamil Nadu using

589 DSAS and geospatial technology. *Environmental Earth Sciences*, 71(10): 4523-4542

590 Kuang C P, Chen W, Gu J, He L L (2014). Comprehensive analysis on the sediment siltation in the

591 upper reach of the deepwater navigation channel in the Yangtze Estuary. *Journal of*
592 *Hydrodynamics*, 26(2): 299-308

593 Latrubesse E M (2008). Patterns of anabranching channels: The ultimate end-member adjustment
594 of mega rivers. *Geomorphology*, 101(1-2): 130-145

595 Li M T, Chen Z Y, Yin D W, Chen J, Wang Z H, Sun Q L (2011). Morphodynamic characteristics of
596 the dextral diversion of the Yangtze River mouth, China: tidal and the Coriolis Force controls.
597 *Earth Surface Processes and Landforms*, 36(5): 641-650

598 Li M T, Ge J Z, Kappenberg J, Much D, Nino O, Chen Z Y (2014). Morphodynamic processes of
599 the Elbe River estuary, Germany: the Coriolis effect, tidal asymmetry and human dredging.
600 *Frontiers of Earth Science*, 8(2): 181-189

601 Li Z W, Yu G A, Brierley G, Wang Z Y (2016). Vegetative impacts upon bedload transport capacity
602 and channel stability for differing alluvial planforms in the Yellow River source zone. *Hydrology*
603 *and Earth System Sciences*, 20(7): 3013-3025

604 Liu F, Hu S, Guo X J, Luo X X, Cai H Y, Yang Q S (2018). Recent changes in the sediment regime
605 of the Pearl River (South China): Causes and implications for the Pearl River Delta.
606 *Hydrological Processes*, 32(12): 1771-1785

607 Luan H L, Ding P X, Wang Z B, Ge J Z, Yang S L (2016). Decadal morphological evolution of the
608 Yangtze Estuary in response to river input changes and estuarine engineering projects.
609 *Geomorphology*, 265: 12-23

610 Mendoza A, Soto-Cortes G, Priego-Hernandez G, Rivera-Trejo F (2019). Historical description of
611 the morphology and hydraulic behavior of a bifurcation in the lowlands of the Grijalva River
612 Basin, Mexico. *Catena*, 176: 343-351

613 Ni B, He R, Zhang W (2014). Study on dredging scale of Tongzhousha west channel. *Journal of*
 614 *Waterway and Harbor*, 35(6): 608-612 (in Chinese)
 615 Petts G E, Gurnell A M (2005). Dams and geomorphology: Research progress and future directions.
 616 *Geomorphology*, 71(1-2): 27-47
 617 Rangoonwala A, Jones C E, Ramsey E (2016). Wetland shoreline recession in the Mississippi River
 618 Delta from petroleum oiling and cyclonic storms. *Geophysical Research Letters*, 43(22): 11652-
 619 11660
 620 Schletterer M, Shaporenko S I, Kuzovlev V V, Minin A E, Van Geest G J, Middelkoop H, Gorski K
 621 (2019). The Volga: Management issues in the largest river basin in Europe. *River Research and*
 622 *Applications*, 35(5): 510-519
 623 Shen Y M, Deng G F, Xu Z H, Tang J (2019). Effects of sea level rise on storm surge and waves
 624 within the Yangtze River Estuary. *Frontiers of Earth Science*, 13(2): 303-316
 625 Sloff K, Van Spijk A, Stouthamer E, Sieben A (2013). Understanding and managing the morphology
 626 of branches incising into sand-clay deposits in the Dutch Rhine Delta. *International Journal of*
 627 *Sediment Research*, 28(2): 127-138
 628 Sun J L, Lei X H, Tian Y, Liao W H, Wang Y H (2013). Hydrological impacts of climate change in
 629 the upper reaches of the Yangtze River Basin. *Quaternary International*, 304: 62-74
 630 Wang Y H, Dong P, Oguchi T, Chen S L, Shen H T (2013). Long-term (1842-2006) morphological
 631 change and equilibrium state of the Changjiang (Yangtze) Estuary, China. *Continental Shelf*
 632 *Research*, 56: 71-81
 633 Warne A G, Guevara E H, Aslan A (2002). Late Quaternary evolution of the Orinoco Delta,
 634 Venezuela. *Journal of Coastal Research*, 18(2): 225-253

635 Wu Z G, Chen Y P, Zhang C K, Jiang N L (2013). Fluvial dynamic analysis of Rugaosha reach in
636 Changjiang Estuary. *Yangtze River*, 44(24): 13-16+19 (in Chinese)

637 Xu Y, Gong H F, Zhang H (2014). Study on branch selection for 12.5 m - deep main channel in
638 Fujiangsha reach downstream the Changjiang River. *Port & Waterway Engineering*, 2014(5): 1-
639 7 (in Chinese)

640 Yang S L, Milliman J D, Li P, Xu K (2011). 50,000 dams later: Erosion of the Yangtze River and its
641 delta. *Global and Planetary Change*, 75(1-2): 14-20

642 Yang S L, Xu K H, Milliman J D, Yang H F, Wu C S (2015). Decline of Yangtze River water and
643 sediment discharge: Impact from natural and anthropogenic changes. *Scientific Reports*, 5:
644 12581

645 Yang X W, Lin Q (2013). Evolution analysis and maintenance countermeasures of north channel of
646 Fujiang shoal in Lower Yangtze River. *Journal of Waterway and Harbor*, 34(1): 50-54 (in
647 Chinese)

648 Yu W C, eds (2013). *Understanding and Practice of the Yangtze River*. Beijing: China Water &
649 Power Press (in Chinese)

650 Yun C X, eds (2004). *Recent Developments of the Changjiang Estuary*. Beijing: China Ocean Press
651 (in Chinese)

652 Zeng X F, Zhao N, Zhou J Z (2013). Study on hydropower energy and its future changes in the
653 upper Yangtze River basin under climate change. *Advanced Research on Material, Energy and*
654 *Control Engineering*, 648: 232-236

655 Zhang W, Xu P (2017). Morphological relationships of runoff tidal estuary on the lower reaches of
656 the Yangtze River. *China Harbour Engineering*, 37(1): 19-23 (in Chinese)

- 657 Zhang W, Xu Y, Hoitink A J F, Sassi M G, Zheng J H, Chen X W, Zhang C (2015). Morphological
658 change in the Pearl River Delta, China. *Marine Geology*, 363: 202-219
- 659 Zhao J, Guo L C, He Q, Wang Z B, van Maren D S, Wang X Y (2018). An analysis on half century
660 morphological changes in the Changjiang Estuary: Spatial variability under natural processes
661 and human intervention. *Journal of Marine Systems*, 181: 25-36
- 662 Zheng S W, Cheng H Q, Shi S Y, Xu W, Zhou Q P, Jiang Y H, Zhou F N, Cao M X (2018). Impact
663 of anthropogenic drivers on subaqueous topographical change in the Datong to Xuliujing reach
664 of the Yangtze River. *Science China - Earth Sciences*, 61(7): 940-950
- 665 Zhou Y Y, Huang H Q, Ran L S, Shi C X, Su T (2018). Hydrological controls on the evolution of
666 the Yellow River Delta: An evaluation of the relationship since the Xiaolangdi Reservoir became
667 fully operational. *Hydrological Processes*, 32(24): 3633-3649
- 668 Zhu B Y, Deng J Y, Yue Y, Li Z W, Zhang C C (2019). Responses of erosion and deposition in
669 braided reaches between Datong and Jiangyin to varying water and sediment discharges in lower
670 Yangtze River. *Taiwan Water Conservancy*, 67(2): 46-57 (in Chinese)
- 671 Zhu B Y, Li Y T, Yang P Y, Deng J Y, Yang Y P, Li S X (2018). River bed erosion and deposition
672 responses to sediment reduction in the Chengtong reach of the Yangtze River. *Advances in Water
673 Science*, 29(5): 706-716 (in Chinese)
- 674 Zhu B Y, Li Y T, Yue Y, Yang Y P (2017). Aggravation of north channels' shrinkage and south
675 channels' development in the Yangtze Estuary under dam-induced runoff discharge flattening.
676 *Estuarine Coastal and Shelf Science*, 187: 178-192

677 **Author biographies**

678  Boyuan ZHU

679 Water Conservancy and Hydropower Engineering, B.S., Wuhan University, Wuhan,
680 China, 2011

681 Hydraulics and River Dynamics, Ph.D, Wuhan University, Wuhan, China, 2017

682 Dr. Zhu served as a technical professional in Zhongnan Engineering Corporation
683 Limited of Power China during 2017-2018, before taking up a teaching position at
684 Changsha University of Science & Technology from 2018. His research interests
685 include sediment transport and river evolution.

686 The email address of Dr. Zhu is: boyuan@csust.edu.cn

687 **□ Jinyun DENG**

688 Port, Channel and River Regulation, B.S., Wuhan University, Wuhan, China, 1998

689 Hydraulics and River Dynamics, M.S., Wuhan University, Wuhan, China, 2000

690 Hydraulics and River Dynamics, Ph.D, Wuhan University, Wuhan, China, 2003

691 Prof. Deng gained a teaching position in Wuhan University in 2003 and was
692 appointed associate professor in 2006. His research interests include sediment
693 transport and river evolution.

694 The email address of Prof. Deng is: dengjinyun@whu.edu.cn

695 **□ Jinwu TANG**

696 Port, Channel and River regulation, B.S., Wuhan University, Wuhan, China, 2007

697 Hydraulics and River Dynamics, Ph.D, Wuhan University, Wuhan, China, 2012

698 Dr. Tang is a technical professional in Changjiang Institute of Survey, Planning,
699 Design and Research, where he has been employed since 2012. His research
700 interests include river planning and management.

701 The email address of Dr. Tang is: tangjinwu1106@163.com

702 **□ Wenjun YU**

703 Water Conservancy and Hydropower Engineering, B.S., Xi'an University of
704 Technology, Xi'an, China, 2012

705 Hydraulics and River Dynamics, M.S., Wuhan University, Wuhan, China, 2015

706 Mr. Yu is a technical professional in Changjiang Waterway Institute of Planning,
707 Design & Research, where he has been employed since 2015. His research interests
708 include river regulation and management.

709 The email address of Mr. Yu is: y430011@sina.cn

710 **□ Alistair G.L. BORTHWICK**

711 Civil engineering, BEng (1st class), University of Liverpool, Liverpool, UK, 1978

712 PhD, University of Liverpool, Liverpool, UK, 1982

713 MA, University of Oxford, Oxford, UK, 1990

714 DSc, University of Oxford, Oxford, UK, 2007

715 Prof. Borthwick was previously professor of engineering science at the University
716 of Oxford, where he worked for 21 years from 1990-2011. He is presently a
717 professorial fellow at the University of Edinburgh. His research interests include
718 coastal and offshore engineering, environmental fluid mechanics, and marine
719 power resource assessment.

720 Prof. Borthwick has 40 years' engineering, research, and teaching experience. He
721 was elected a Fellow of the Institution of Civil Engineers, FICE, in 2003, a Fellow
722 of the Royal Academy of Engineering, FREng, in 2014, and a Fellow of the Royal

723 Society of Edinburgh, FRSE, in 2015.

724 His email address is: Alistair.Borthwick@ed.ac.uk

725 **□ Yuanfang CHAI**

726 Agricultural Water Conservancy Engineering, B.S., Taiyuan University of

727 Technology, Taiyuan, China, 2016

728 Hydraulics and River Dynamics, M.S., Wuhan University, Wuhan, China, 2019

729 Mr. Chai's research interests include sediment transport and river evolution.

730 His email address is: 2808676930@qq.com

731 **□ Zhaohua SUN**

732 Port, Channel and River Regulation, B.S., Wuhan University, Wuhan, China, 1999

733 Hydraulics and River Dynamics, Ph.D, Wuhan University, Wuhan, China, 2004

734 Prof. Sun took up a teaching position in Wuhan University in 2004 and has since

735 been appointed associate professor. His research interests include sediment

736 transport and river evolution.

737 His email address is: Lnszh@126.com

738 **□ Yitian LI**

739 Port, Channel and River Regulation, B.S., Wuhan University, Wuhan, China, 1981

740 Hydraulics and River Dynamics, Ph.D, Wuhan University, Wuhan, China, 1987

741 Prof. Li has been employed by Wuhan University for 32 years, where he is senior

742 professor in river engineering. His research interests include sediment transport and

743 river evolution.

744 Prof. Li is vice director of the Sediment Committee of the Chinese Hydraulic

745 Engineering Society. He has won two Second Class Prizes for the Scientific and
746 Technological Progress of China. His email address is: ytli@whu.edu.cn
747